# Mantle volatiles and heat contributions in high sulfidation epithermal deposit from the Zijinshan Cu-Au-Mo-Ag orefield, Fujian Province, China: Evidence from He and Ar isotopes

Li-Yan Wu[a], Rui-Zhong Hu[a,*], Xiao-Feng Li[a,b], Finlay M. Stuart[a,c], Guo-Hao Jiang[a], You-Qiang Qi[a], Jing-Jing Zhu[a]

[a] State Key Laboratory of Ore Deposit Geochemistry, Institute of Geochemistry, Chinese Academy of Sciences, Guiyang 550002, China
[b] Key Laboratory of Mineral Resources, Institute of Geology and Geophysics, Chinese Academy of Sciences, Beijing 100029, China
[c] Scottish Universities Environmental Research Centre, Scottish Enterprise Technology Park, Rankine Avenue, East Kilbride G75 0QF, UK

## ARTICLE INFO

## ABSTRACT

The source of metal and sulphur in porphyry and related epithermal deposits is a long debated issue. The role of mantle-derived magmas in providing the metals has proved particularly problematic. Here we report new He and Ar isotope determinations from ore fluids from the Zijinshan high sulfidation-epithermal Cu-Au deposit and Wuziqilong transitional Cu deposit from the giant Zijinshan porphyry-epithermal Cu-Au-Mo-Ag ore system (from 105 to 91 Ma), to decipher the contribution of mantle-derived volatiles and heat. Hydrothermal fluids in pyrite and digenite have $^3He/^4He$ up to 5.7 $R_a$, among the highest measured in ancient ore-forming fluids. A linear correlation between He and Ar isotopes indicate that the ore fluids were, to a first order, a mixture between a shallow crustal fluid, with low $^3He/^4He$, and a dominantly mantle-derived fluid with high $^3He/^4He$. The mantle $^3He/^4He$ is close to values typical of the upper mantle indicating the initial magmas that provided the heat for hydrothermal systems did not assimilate large volumes of continental crust. The ore-forming fluids have $^3He/$ heat ratios that are 10 to 80 times higher than that of mid-oceanic ridge hydrothermal fluids, indicating that the metal-bearing fluids acquired heat and volatiles in a convective, rather than conductive, hydrothermal regime. It appears that mantle-derived volatiles, heat and probably metals have made a major contribution to the Cu-Au-Mo-Ag mineralization in the Zijinshan orefield.

## 1. Introduction

The source of metals and sulphur in porphyry mineralization and related epithermal deposits has been debated for several decades. The magmatic $\delta^{34}S$ of sulfide minerals from many porphyry deposits (Eastoe, 1983; Field and Gustafson, 1976) and meteoric water isotope signatures (Sheppard and Taylor, 1974) led many to consider that the felsic magmas (Burnham, 1979) and/or the surrounding country rocks (Ohmoto and Goldhaber, 1997; Sheppard and Taylor, 1974) are the main source of metals However, the low solubility of sulphur in felsic magmas (Hattori and Keith, 2001;Wallace and Carmichael, 1992) rules them out as suppliers of the metal in the ore-forming systems (Imai et al., 1993; Sillitoe, 1997; Sun et al., 2004). It is likely that mafic magmas play an important role in triggering felsic magmatism, and in generating the conditions necessary to form porphyry deposits (Chiaradia et al., 2012; Hattori, 1993; Hattori and Keith, 2001), especially giant deposits (Porter, 2005). Mafic magmas have great capacity

to transfer sulphur and metal from the mantle to the shallow crust due to the high sulphur solubility (Hattori and Keith, 2001; Sun et al., 2004), which could supply enough metal and S for the porphyry and related epithermal deposits. Understanding the relationship between the mantle melting, felsic magmas and porphyry-epithermal deposits is essential to establishing genetic models of ore deposition.

Noble gas isotopes are unique tracers of the involvement of mantle magmas in the generation of ore deposits (Burnard et al., 1999; Burnard and Polya, 2004; Davidheiser-Kroll et al., 2014; Hu et al., 2012; Kendrick et al., 2001; Stuart et al., 1995; Wu et al., 2011) by virtue of the difference between $^3He/^4He$ of upper mantle (7–9 $R_a$; Graham, 2002, where $R_a$ is the atmospheric $^3He/^4He$ ratio, $1.39 \times 10^{-6}$) and crustal rocks (0.01–0.05 $R_a$; O'Nions and Oxburgh, 1983).

The Zijinshan orefield is a unique and giant Cu-Au-Mo-Ag ore system that includes several major porphyry, high sulfidation (HS)- and low sulfidation (LS)-epithermal, and transitional deposits (Jiang et al., 2013). The mineral deposits are spatially, temporally and genetically
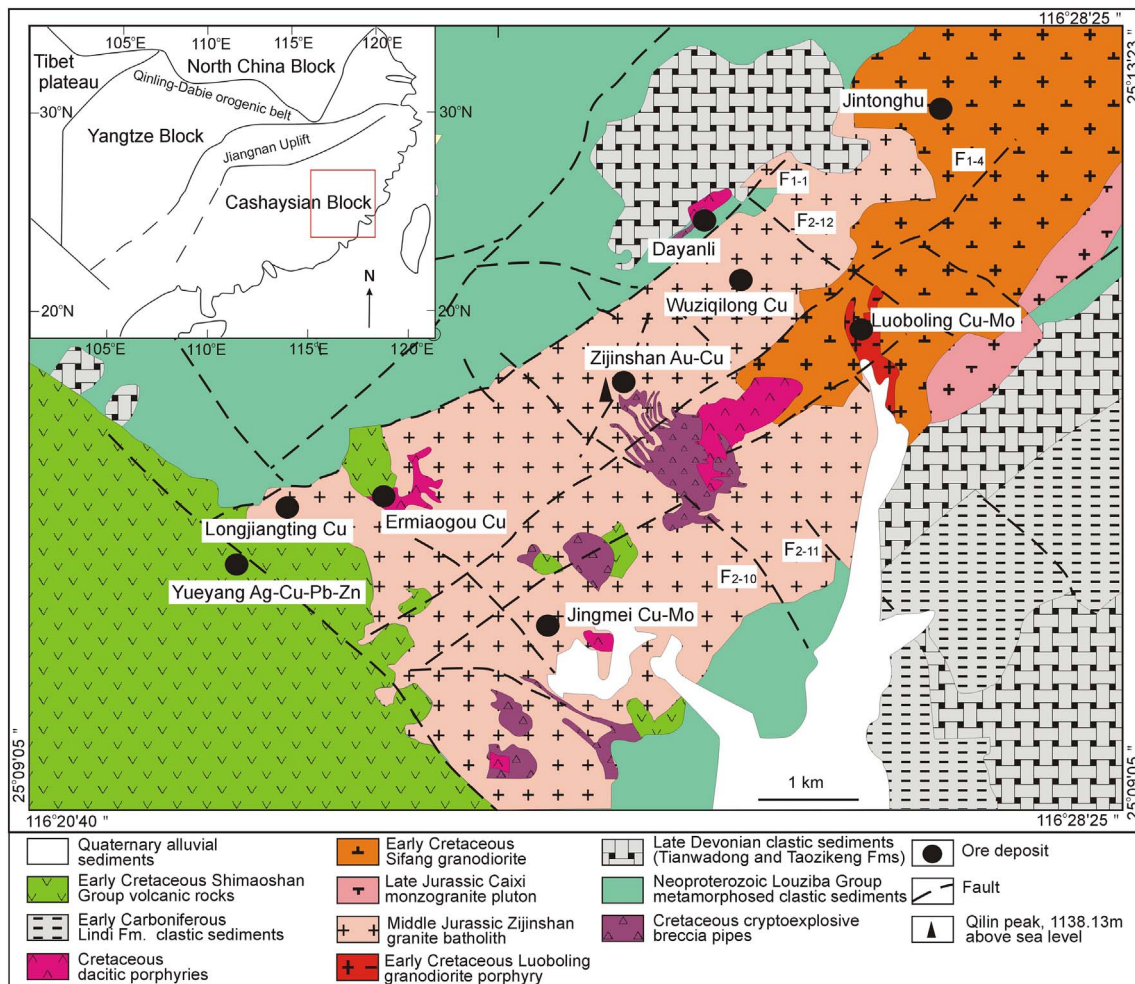
**Fig. 1.** Geological map of the Zijinshan orefield, South China modified from Hu and Zhou (2012) and Zhong et al. (2014).

related to Cretaceous granodiorite and volcanic rocks which are believed to have formed by mixing of mantle-derived magmas with crustal magmas (Jiang et al., 2013; Li and Jiang, 2014). How, and to what extent, mantle melting initiated the felsic magmatism, and drove the ore-forming hydrothermal fluid system are still not clear. Here we present study of the He and Ar isotopic composition of the ore fluids trapped in pyrite and digenite from the Zijinshan high sulfidation Cu–Au deposit and Wuziqilong Cu deposit, in order to reveal the genesis of the deposits and the contribution of mantle-derived volatiles and heat.

Geological background

The Zijinshan ore field is located in the Cathaysian block (Fig. 1) in Fujian Province. The ore field is host to several types of hydrothermal Cu-Au-Mo-Ag deposits (Jiang et al., 2013; Zhang et al., 2003): high-sulfidation epithermal deposit (Zijinshan), porphyry deposit (Luoboling), low-sulfidation epithermal deposit (Yueyang), and a transitional type (Wuziqilong) which share some features with both epithermal and porphyry deposits in the region. The major deposits tend to be located at the intersection of the Xuanhe anticlinorium and Shang-hang-Yunxiao fault zone. Mineralization is likely driven by Mesozoic felsic magmatism (Hu and Zhou, 2012; Mao et al., 2013). Hydrothermal Cu ± Au ore deposits of the Zijinshan are spatially and temporally associated with the Sifang, Luoboling, Zhongliao plutons and dacite porphyry. They are believed to have formed by mixing between mantle-derived magma with crustal magmas (Jiang et al., 2013; Li and Jiang, 2014). The magmatic intrusion and contemporaneous mineralization lasted at least 10 Ma, from 105 Ma to 91 Ma (Jiang et al., 2015 and references therein). By the end of 2008 the region had proven reserves

of 323 t Au ($\sim$ 0.5 g/t), 2.36 Mt. Cu ($\sim$ 0.5 wt%), 1554 t Ag (20–156 g/t), and 4647 t Mo (0.03 wt%) (Zhong et al., 2014).

The Zijinshan high-sulfidation Cu-Au deposit and Wuziqilong Cu deposit mineralization is fault controlled, filling a system of NW-trending fractures (Fig. 1). The hydrothermal alteration and mineralization are typically zoned, including silicic, alunite, dickite and phyllic alteration (So et al., 1998). Intense silification and limonitization are dominant in the leached zone at levels shallower than 350 m in Zijinshan Cu-Au deposit, where it is associated with Au-Ag mineralization (So et al., 1998; Liu et al., 2016). Copper ore bodies occur in the alunite alteration zone, at levels < 650 m, and mineralization is dominated by massive digenite-covellite ore. The mineral assemblage is characterized by the presence of digenite, covellite, enargite, pyrite, alunite, along with trace bornite and chalcopyrite. The mineralization of Wuziqilong Cu deposit is dominated by pyrite and covellite, with minor digenite, bornite, chalcopyrite and luzonite (enargite).

Primary fluid inclusions in gangue quartz deposited during mineralization have homogenization temperatures that range from 160 °C to 380 °C (Zijinshan) and from 230 °C to 570 °C (Wuziqilong), with salinities between 1and 22 wt% NaCl eqv (Zijinshan, So et al., 1998; Zhang et al., 1992) and 0.2–14.7 wt% NaCl eqv (Wuziqilong, Chen et al., 2011). The relationship between homogenization temperatures and salinity indicate that a simple cooling and dilution of the hydrothermal fluids occurred due to the addition of meteoric waters to the hydrothermal fluids (So et al., 1998). The δD and δ$^{18}$O (Zhang et al., 1992) of the ore-forming fluids is consistent with derivation as mixtures of meteoric fluid with magmatic hydrothermal fluid.

**Table 1**
He, Ar and S isotopic compositions of the sulfides from Wuziqilong and Zijinshan deposits.

| Sample | Mineral | Weight (g) | $^4$He ($10^{-8}$ cm$^3$STP) | $^{40}$Ar ($10^{-8}$ cm$^3$STP) | $^3$He/$^4$He ($R_a$) | $^{40}$Ar/$^{36}$Ar | $^3$He/$^{36}$Ar ($10^{-5}$) | $^{40}$Ar*/$^4$He ($10^{-3}$) | $^4$He (cm$^3$ STP g$^{-1}$) | $^{40}$Ar (cm$^3$ STP g$^{-1}$) | $\delta^{34}$S (‰) |
|---|---|---|---|---|---|---|---|---|---|---|---|
| **Wuziqilong** | | | | | | | | | | | |
| WZQL-1 | Pyrite | 0.272 | 18.39 ± 0.28 | 16.11 ± 0.09 | 5.01 ± 0.12 | 385 ± 5 | 3.06 ± 0.10 | 196.8 ± 8.0.0 | 6.77 × 10$^{-7}$ | 5.93 × 10$^{-7}$ | 2.88 ± 0.02 |
| WZQL-3 | Pyrite | 0.341 | 10.41 ± 0.16 | 12.11 ± 0.07 | 2.89 ± 0.08 | 341 ± 3 | 1.18 ± 0.04 | 143.2 ± 4.8 | 3.05 × 10$^{-7}$ | 3.55 × 10$^{-7}$ | 1.82 ± 0.03 |
| WZQL-4 | Pyrite | 0.214 | 4.82 ± 0.07 | 9.29 ± 0.05 | 3.99 ± 0.10 | 342 ± 7 | 0.98 ± 0.04 | 245.4 ± 14.1 | 2.25 × 10$^{-7}$ | 4.34 × 10$^{-7}$ | 1.45 ± 0.10 |
| WZQL-5-2 | Pyrite | 0.407 | 21.81 ± 0.33 | 46.66 ± 0.27 | 5.50 ± 0.14 | 341 ± 3 | 1.22 ± 0.03 | 264.1 ± 8.4 | 5.36 × 10$^{-7}$ | 1.15 × 10$^{-6}$ | 3.23 ± 0.20 |
| WZQL-8 | Pyrite | 0.277 | 19.81 ± 0.30 | 7.09 ± 0.04 | 0.87 ± 0.02 | 315 ± 7 | 1.06 ± 0.04 | 18.2 ± 1.0 | 7.14 × 10$^{-7}$ | 2.55 × 10$^{-7}$ | − 0.26 ± 0.04 |
| WZQL-10 | Pyrite | 0.186 | 6.26 ± 0.10 | 4.81 ± 0.03 | 4.99 ± 0.15 | 405 ± 26 | 3.65 ± 0.33 | 201.5 ± 29.3 | 3.37 × 10$^{-7}$ | 2.59 × 10$^{-7}$ | 0.16 ± 0.08 |
| WZQL-14 | Pyrite | 0.146 | 4.77 ± 0.07 | 1.68 ± 0.01 | 2.63 ± 0.07 | 468 ± 96 | 4.86 ± 1.11 | 127.6 ± 54.5 | 3.27 × 10$^{-7}$ | 1.15 × 10$^{-7}$ | − 0.69 ± 0.06 |
| **Zijinshan** | | | | | | | | | | | |
| ZJS-3 | Pyrite | 0.235 | 7.70 ± 0.12 | 2.46 ± 0.01 | 5.41 ± 0.15 | 612 ± 64 | 14.41 ± 1.84 | 163.7 ± 37.1 | 3.28 × 10$^{-7}$ | 1.05 × 10$^{-7}$ | 3.61 ± 0.08 |
| ZJS-4 | Pyrite | 0.145 | 257 ± 3.95 | 5.62 ± 0.03 | 0.16 ± 0.01 | 482 ± 20 | 4.87 ± 0.32 | 8.30 ± 0.8 | 1.78 × 10$^{-5}$ | 3.87 × 10$^{-7}$ | 3.59 ± 0.03 |
| ZJS-6 | Pyrite | 0.210 | 36.55 ± 0.56 | 19.30 ± 0.11 | 5.67 ± 0.14 | 536 ± 7 | 8.00 ± 0.25 | 233.7 ± 9.3 | 1.74 × 10$^{-6}$ | 9.21 × 10$^{-7}$ | 2.47 ± 0.05 |
| ZJS-36 | Digenite | 0.141 | 2.92 ± 0.04 | 6.20 ± 0.04 | 0.41 ± 0.02 | 320 ± 10 | 0.09 ± 0.01 | 143.8 ± 11.2 | 2.08 × 10$^{-7}$ | 4.41 × 10$^{-7}$ | − 5.83 ± 0.02 |

(1) Sample weights are the < 100 μm fractions after crushing.
(2) Errors quoted are at the 1σ confidence level.
(3) $^{40}$Ar* is non-atmospheric Ar, $^{40}$Ar* = $^{40}$Ar-[$^{36}$Ar × 298.6].

## 1.1. Sampling and analytical methods

The samples used in this study were collected from ~390 m deep within the Wuziqilong Cu mine and ~350 m below the original land surface from the open pit of the Zijinshan high-sulfidation Cu-Au deposit. All samples are from veins and are mostly euhedral crystals. Pure pyrite (1–3 mm) was picked from the crushed ore under a binocular microscope. The analytical methods used here were similar to those described in Hu et al. (2012). Approximately 0.5–1 g of 0.8–1.5 mm grains were cleaned ultrasonically in alcohol. The dried samples were loaded to an in vacuo crusher comprised of modified Nupro-type valves (Stuart et al., 1994b) and baked at ~150 °C at ultra-high vacuum for > 24 h to remove adhered atmospheric gases. Sample weights reported in Table 1 are the fraction which passed through a 100 μm sieve after crushing. The volatiles in fluid inclusions were extracted by sequential crushing, and exposed to a titanium-sponge furnace at 800 °C for 20 min to remove active gases such as $H_2O$ and $CO_2$, and then to two SAES Zr-Al getters at lower temperatures (250 °C and room temperature) each for 10 min. Argon was separated from the remaining gas by exposure to activated charcoal cooled by liquid $N_2$ (− 196 °C) for 40 min. Helium and argon isotopes were determined using a GV5400 mass spectrometer. Mass spectrometer sensitivity and mass fractionation were determined by repeated measurements of air. Crush blanks were < 2 × 10$^{-10}$ cm$^3$ STP $^4$He and < 4 × 10$^{-10}$ cm$^3$ STP $^{40}$Ar, which are two orders of magnitude less than those of the samples and the air standard.

The sulphur isotope composition of the sulfide minerals was determined using a MAT253 continuous flow isotope ratio mass spectrometer coupled to an elemental analyzer (EA-IRMS) at the State Key Laboratory of Ore Deposit Geochemistry Institute of Geochemistry, Chinese Academy of Sciences. Measurements are reported using standard δ-notation relative to V-CDT international standard. The reproducibility of replicate analyses of the IAEA international standards: IAEA S1 (− 0.3‰), IAEA S2 (+ 22.62‰) and IAEA S3 (− 32.49‰) yields a precision that is better than 0.2‰ (1σ).

## 2. Results

The He, Ar and S isotopic compositions of pyrite and digenite separates of the Wuziqilong Cu deposit and Zijinshan high sulfidation Cu-Au deposit are listed in Table 1. The large range of the abundance of $^4$He and $^{40}$Ar (2.1–178 × 10$^{-7}$ cm$^3$ STP g$^{-1}$ and 1.1–11.5 × 10$^{-7}$ cm$^3$ STP g$^{-1}$, respectively) are likely due to variation in the volume of fluid inclusions in the samples, and variable crushing efficiency. $^3$He/$^4$He ratios of the ore fluids vary from 0.87 to 5.5 $R_a$ (Wuziqilong) and 0.16 to 5.7 $R_a$ (Zijinshan). The highest ratios from each deposit are among the highest values recorded for ancient ore-forming fluids. $^{40}$Ar/$^{36}$Ar vary from 315 to 468 (Wuziqilong) and from 320 to 612 (Zijinshan). Zijinshan pyrite and digenite $\delta^{34}$S range from − 5.83 to + 3.61‰, while the Wuziqilong pyrite $\delta^{34}$S range from − 0.69 to + 3.23‰.

## 3. Discussion

### 3.1. Post-entrapment modifications of fluid inclusions

Several processes may affect the He and Ar isotope composition since mineral crystallisation such that the crush-released volatiles may not reflect the composition of the fluid inclusions. Cosmogenic He (e.g. Foeken et al. 2009) can be ruled out as all samples were taken from significantly below the Earth surface. U and Th concentrations in hydrothermal fluids are commonly low (Hu et al., 2012; Normal and Musgrave, 1994), therefore the radiogenic $^4$He produced in situ in fluid inclusions is also negligible (Hu et al., 2012). Trace amounts of U and Th in mineral structures may produce in situ radiogenic $^4$He. However, empirical observations provide no evidence that significant volumes of
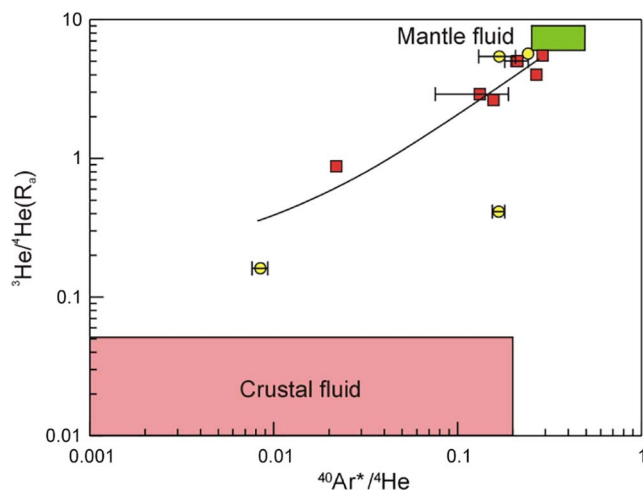
Fig. 2. $^{40}Ar*/^4He$ vs. $^3He/^4He$ ($R_a$) of sulfides from the Zijinshan high sulfidation Cu-Au deposit and Wuziqilong Cu deposit. Symbols: red filled squares: Wuziqilong transitional Cu deposit; yellow filled circles: Zijinshan HS Cu-Au deposit. The linear correlation is obtained by least squares regression: $^3He/^4He$ (Ra) = 21.0 × $^{40}Ar*/^4He$ + 0.07, $r^2$ = 0.69. Error bars not displayed are concealed in the sample symbols, as follows. (For interpretation of the references to colour in this figure legend, the reader is referred to the web version of this article.)

radiogenic He diffuses or recoils into or out of fluid inclusions in ore minerals (Stuart et al., 1995; Burnard and Polya, 2004).

The $^{40}Ar$ produced by the decay of K in fluid inclusions and the host mineral such as pyrite are also negligible, because the diffusion of Ar in pyrite and the concentrations of K are extremely low (Smith et al., 2001; York et al., 1982). The measured $^{40}Ar/^{36}Ar$ of the volatiles released from fluid inclusions are likely lower than the true fluid value due to the release of atmospheric Ar (Burnard et al., 1999).

### 3.2. Sources of He, Ar and S

The most important sources of He and Ar in ore fluid inclusions trapped in hydrothermal minerals are air-saturated water, mantle-derived volatiles and radiogenic decay of U, Th and K in crustal rocks (Turner et al., 1993; Stuart et al., 1995). Helium in the atmosphere is too low to exert a significant influence on the abundance and isotopic compositions of He in most crustal fluids thus it is predominantly mantle-derived and crustal-radiogenic in origin (Stuart et al., 1994a). This is supported by the high $^4He/^{36}Ar$ of the fluids (151 to 22,131, the atmospheric $^4He/^{36}Ar$ = 0.167). The $^3He/^4He$ ratios of the sulfide fluids from the two deposits (0.16–5.67 $R_a$; Table 1 Figs. 2, 3) are consistent with an origin as a mixture of crustal radiogenic (0.01–0.05 $R_a$; O'Nions and Oxburgh, 1983) and mantle component, which could be upper mantle (7–9 $R_a$; Graham, 2002) and/or subcontinental lithospheric mantle (SCLM, 6–7 $R_a$; Gautheron and Moreira, 2002) sources.

All $^{40}Ar/^{36}Ar$ are in excess of the air ratio indicating the presence of radiogenic $^{40}Ar$ in the fluids. Radiogenic Ar in ore-forming fluids originates from both crust and mantle (e.g. Stuart et al. 1995). The linear correlations between $^3He/^4He$ and $^{40}Ar*/^4He$ (where $^{40}Ar*$ is non-atmospheric Ar, i.e. $^{40}Ar* = ^{40}Ar - [^{36}Ar \times 298.6]$) (Fig. 2), and between $^3He/^{36}Ar$ and $^{40}Ar/^{36}Ar$ (Fig. 3) indicate that the sulfide-hosted volatiles from both deposits are mixtures of two fluids; a high $^3He/^4He$-$^{40}Ar/^{36}Ar$ component and a low $^3He/^4He$-$^{40}Ar/^{36}Ar$ component. These reflect mantle-derived magmatic gases and crust-derived gases, respectively (e.g. Stuart et al. 1995). This may be reflected in the occurrence of two types of fluid inclusions in the quartz associated with sulfides in the deposits, namely high temperature-salinity magmatic-hydrothermal fluids and low temperature-salinity fluids (Chen et al., 2011; So et al., 1998; Zhang et al., 1992).

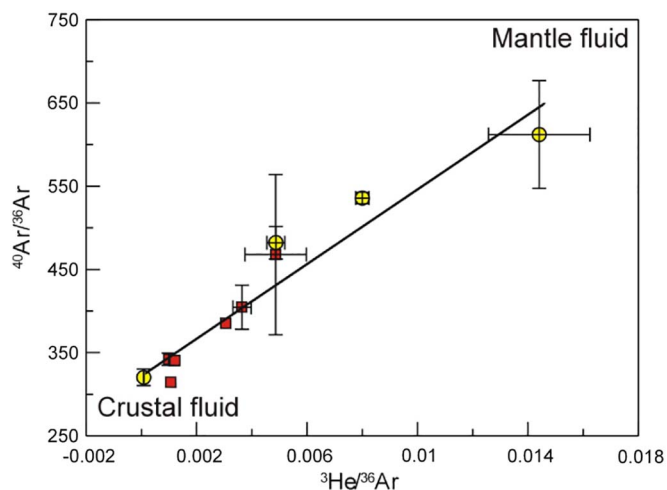The crustal volatiles are likely present in meteoric waters that



Fig. 3. $^3He/^{36}Ar$ vs. $^{40}Ar/^{36}Ar$ of sulfides from the Zijinshan high sulfidation Cu-Au deposit and Wuziqilong Cu deposit. The linear correlation is obtained by least squares regression: $^{40}Ar/^{36}Ar = 0.2 \times 10^{-5} \times ^3He/^{36}Ar + 324$, $r^2$ = 0.92. Symbols as for Fig. 2.

originated at the surface, which has been modified by the addition of radiogenic $^4He$ and $^{40}Ar$. This is termed modified air saturated water (MASW). In Fig. 3, extrapolating the data trend to the $^3He/^{36}Ar$ value of air-saturated water (2.4 × $10^{-7}$) suggests that the MASW component had a $^{40}Ar/^{36}Ar$ ~ 325, slightly higher than atmosphere value (298.6; Lee et al., 2006). Extrapolating the mixing line in Fig. 2 to a $^3He/^4He$ of crustal radiogenic He (~0.02 $R_a$; O'Nions and Oxburgh, 1983) implies that the fluid had $^{40}Ar*/^4He$ < 0.0001 (Fig.2). This is significantly lower than the $^{40}Ar*/^4He$ produced in the crust (~0.2, Torgersen et al., 1988), and is consistent with observations that the shallow fluids contain little radiogenic $^{40}Ar$. Extrapolating this trend to $^3He/^4He$ = 5.67 $R_a$, the highest value of the ore-forming fluid, implies that the magma had a $^{40}Ar*/^4He$ ratio of 0.27. This is within the range of mantle production ratios (0.24–0.63, Graham, 2002). The $^3He/^{40}Ar*$ ratio of the samples range from 2.3–6.7 × $10^{-5}$, close to that of MORB mantle value (~$10^{-4}$, Kennedy et al., 1991) and 200–600 times of that of the crust value (~$10^{-8}$, Kennedy et al., 1991), indicating a dominantly mantle origin of He and Ar. The absence of significant contribution of crust-derived radiogenic He and Ar, therefore implies that the volume of crustal magma in the deep ore system was low in comparison to the mantle magma.

The $\delta^{34}S$ values of sulfides from the Zijinshan and Wuziqilong deposits have a large range (−5.8 to +3.6‰; Table 1 and Fig. 5). While this range overlaps the magmatic value (0 ± 2‰; Kyser, 1990), it is not particularly diagnostic, and certainly requires other S sources, or significant fractionation during deposition. The sulfides with high $^3He/^4He$ ratio have $\delta^{34}S$ range from 0.16‰ to 3.61‰, which is consistent with the $\delta^{34}S$ values of the 21°N East Pacific Rise and Mid-Atlantic Ridge sulfides (+1‰ to +3.5‰, Stuart et al., 1994a), indicating mantle origin. The decrease of $\delta^{34}S$ with low $^3He/^4He$, $^{40}Ar/^{36}Ar$, $^3He/^{36}Ar$ and high $^4He/^{40}Ar$ ratios (Fig. 5) indicate a common origin for the radiogenic He and isotopically light S. However the absence of a linear relationship between $\delta^{34}S$ and the He-Ar isotopes (Fig. 5) indicates that the S isotope systematics have not been controlled by the type of fluid mixing that is traced by the noble gases. This most likely reflects the low S concentration in the shallow, low temperature aqueous fluid in comparison to that of the magmatic-hydrothermal fluid.

### 3.3. Helium and heat

The high concentration of mantle-derived $^3He$ in the ore-forming fluids implies that the bulk of the heat (Q) for the main phase of hydrothermal activity derived from the mantle. The $^3He/Q$ ratio of the

fluids can provide constraints on the hydrothermal regime. Following the method of Turner and Stuart (1992) we have:

$$^3He/Q = {}^3He/{}^{36}Ar \times [{}^{36}Ar]_{masw}/(C_p\theta) \qquad (1)$$

where $[{}^{36}Ar]_{masw}$ is the concentration of $^{36}Ar$ in modified air saturated water (MASW, $7.65 \times 10^{-7}$ cm$^3$ STP g$^{-1}$), Cp is the specific heat of MASW (4.4 J K$^{-1}$ g$^{-1}$) and θ is the temperature increase of the cold fluid (°C) (Burnard et al., 1999, Burnard and Polya, 2004). $^3He/Q$ ratios are minima as the presence of atmosphere-derived Ar tends to decrease the $^3He/{}^{36}Ar$, because the He abundance in air is low, so air contamination does not significantly affect He analyses, but air-derived contaminants may comprise a significant fraction of measured Ar, and it is impossible to distinguish fluid-derived Ar from absorbed atmospheric Ar (Burnard et al., 1999). Although rigorous analytical procedures can minimise atmospheric contamination, it is unlikely to completely eliminate air-derived noble gas. Fluid inclusion homogenization temperatures in coexisting gangue minerals of the same mineralizing stage (Chen et al., 2011; So et al., 1998; Zhang et al., 1992) are used to calculate θ in Eq. (1).

The estimated $^3He/Q$ ratio of the fluids from the Zijinshan and Wuziqilong deposits range from 0.07 to $8.35 \times 10^{-12}$ cm$^3$ STP J$^{-1}$ (Fig. 4). These values are 10 to 80 times higher than those recorded by hydrothermal fluids from mid-oceanic ridges ($0.1$–$0.2 \times 10^{-12}$ cm$^3$ STP J$^{-1}$) (Baker and Lupton, 1990; Lupton et al., 1989), though notably they are similar to the values recorded for trapped ore fluids from the Mesozoic granite-related Panasqueria Sn-W mineralisation (Burnard and Polya, 2004). The large variations in $^3He$/heat between samples cannot be accounted for by variable atmospheric $^{36}Ar$ addition and the uncertainties of θ. These variations reflect real changes in the $^3He$ contents and enthalpies of the fluids at the time of trapping (Burnard et al., 1999). The high $^3He/Q$ suggests that the deep hydrothermal fluids derived both heat and volatiles by convection across magma/hydrothermal interface in the deep crust, rather than in a conductive regime (Burnard and Polya, 2004). Meanwhile the near MORB mantle $^3He/{}^{40}Ar^*$ ratio indicate that convective transport of gases from the mantle.

Ore formation at the Zijinshan ore field likely occurred over ~10 Ma between 105 and 91 Ma (Liang et al., 2012, Liu and Hua,
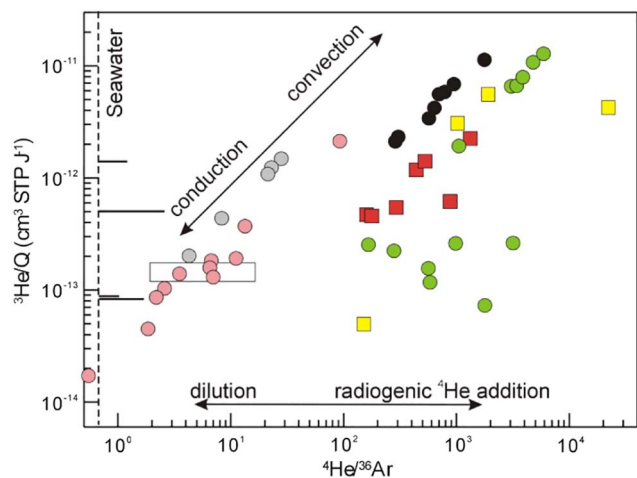
**Fig. 4.** $^3He/Q$ vs. $^4He/{}^{36}Ar$ for sulfides from the Zijinshan high sulfidation Cu-Au deposit and Wuziqilong Cu deposit. Symbols: red filled squares = Wuziqilong deposit; yellow filled squares = Zijinshan deposit; filled circles = Panasqueira aresenopyrite (Burnard and Polya, 2004); green filled circles = Ailaoshan Au deposit (Burnard et al., 1998); gray filled circle = East Pacific Rise sulfides (Turner and Stuart, 1992); pink filled circles = Iceland hydrothermal fluids (Poreda and Arnorsson, 1992); solid horizontal lines = range in $^4He/{}^{36}Ar$ of EPR vent fluids and plumes (Lupton et al., 1989; Lupton et al., 1995); box = Lucky Strike vent fluids (Jean-Baptiste et al., 1998). (For interpretation of the references to colour in this figure legend, the reader is referred to the web version of this article.)
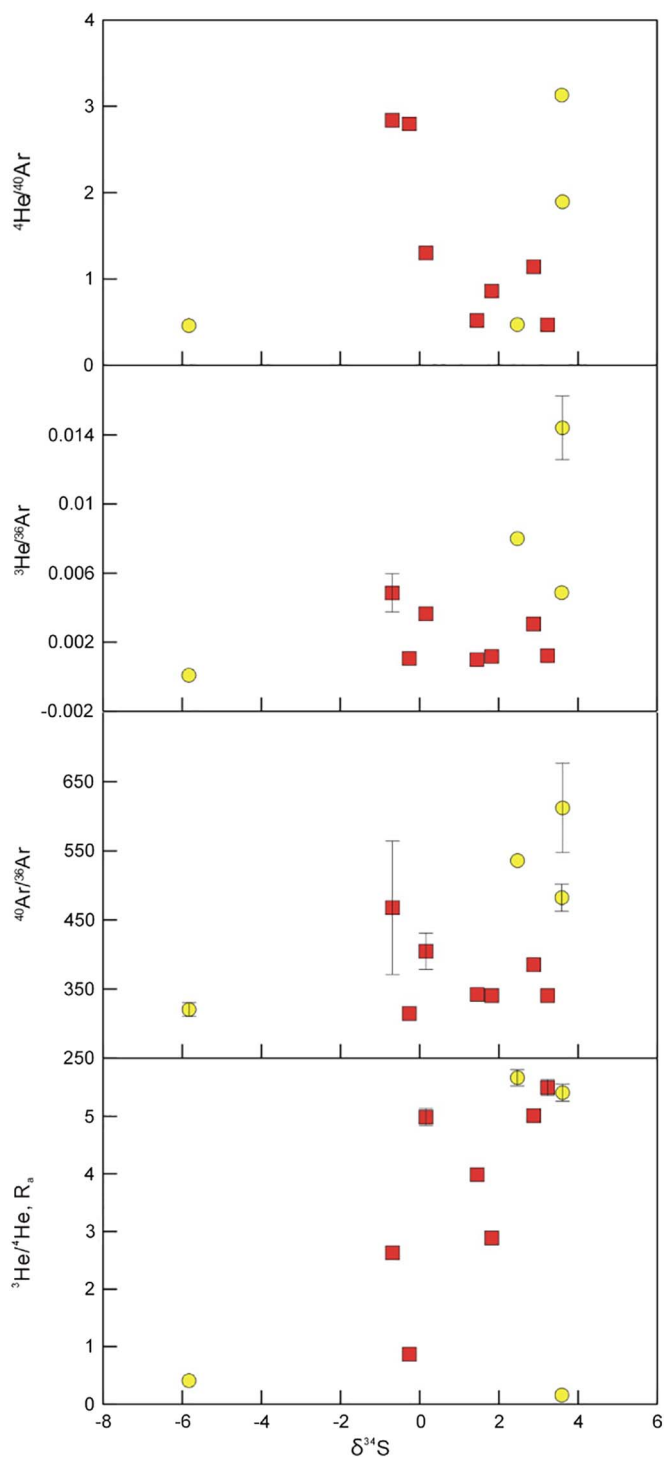
**Fig. 5.** $^3He/{}^4He$ vs. $\delta^{34}S$, $^{40}Ar/{}^{36}Ar$ vs. $\delta^{34}S$, $^3He/{}^{36}Ar$ vs. $\delta^{34}S$, and $^4He/{}^{40}Ar$ vs. $\delta^{34}S$ for sulfides from the Zijinshan high sulfidation Cu-Au deposit and Wuziqilong Cu deposit. There is a poor relationship between S and He-Ar isotopes, though the decrease of $\delta^{34}S$ with low $^3He/{}^4He$, $^{40}Ar/{}^{36}Ar$, $^3He/{}^{36}Ar$ and high $^4He/{}^{40}Ar$ ratios. Symbols as for Fig. 2.

2005). This is considerably longer than the length of time a single intrusion can sustain hydrothermal circulation (~$5 \times 10^5$ yr; Hayba and Ingebritsen, 1997). This requires several pulses of mantle-derived heat in order to ensure a productive hydrothermal system, consistent with the intrusion of multiple plutons (Jiang et al., 2013; Li and Jiang, 2014; Wu et al., 2013).
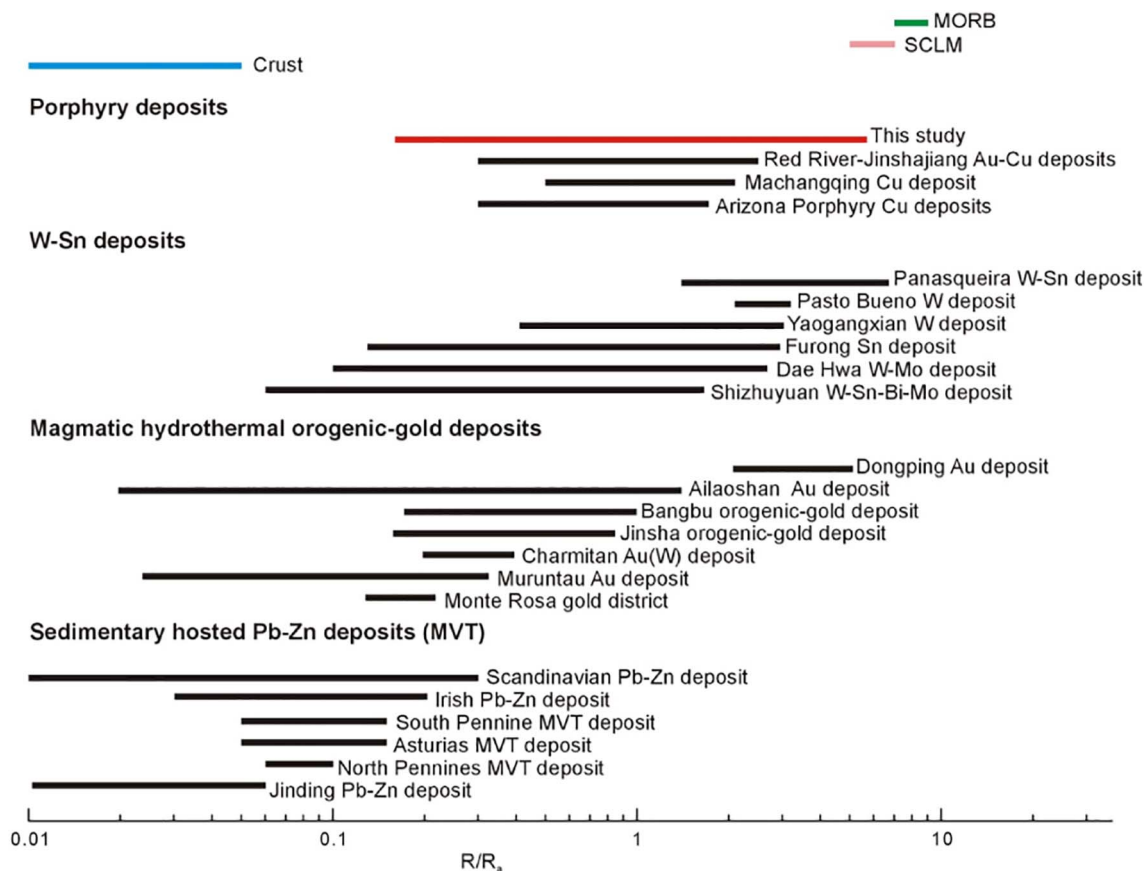
**Fig. 6.** $^3$He/$^4$He of different types of ore deposits (data from Burnard et al., 1999; Burnard and Polya, 2004; Davidheiser-Kroll et al., 2014; Gautheron and Moreira, 2002; Graupner et al., 2006, 2010; Hu et al., 1998a, 1998b, 2004, 2012; Kendrick et al., 2001, 2002, 2005; Li et al., 2007, 2010; Mao and Li, 2003; Morelli et al., 2007; Pettke et al., 1997; Simmons et al., 1987; Stuart and Turner, 1992; Stuart et al., 1995; Sánchez et al., 2010; Tang et al., 2017; Wei et al., 2010; Wu et al., 2011). Most porphyry deposits have $^3$He/$^4$He ratios lower than 2.5 $R_a$, while deposits from Zijinshan orefield have $^3$He/$^4$He ratios up to 5.7 $R_a$. Most W-Sn deposits have $^3$He/$^4$He ratios between 0.06 and 3.2 $R_a$, but there is an exception of Panasqueira W-Cu (Ag)-Sn deposit which has $^3$He/$^4$He ratios up to 6.7 $R_a$. Most magmatic hydrothermal orogenic-gold deposits have $^3$He/$^4$He ratios lower than 1.42 $R_a$, but with an exception of Dongping orogenic-gold deposit from Hebei Province, China, with $^3$He/$^4$He ratios up to 5.2 $R_a$. Most sedimentary hosted Pb-Zn deposits (MVT) share $^3$He/$^4$He ratios lower than 0.3$R_a$. (For interpretation of the references to colour in this figure legend, the reader is referred to the web version of this article.)

### 3.4. Genesis of the ore deposits

Most hydrothermal ore fluids have $^3$He/$^4$He ratios that reflect mixing of shallow and deep magmatic fluids (Hu et al., 2004, 2009, 2012; Stuart et al., 1995; Wu et al., 2011). In most cases $^3$He/$^4$He are lower than 3 $R_a$ (Fig. 6) demonstrating the importance of crust-derived fluids in the genesis of ore deposits. The $^3$He/$^4$He of the Zijinshan and Wuziqilong deposits contrasts with, in particular, other porphyry deposits (Fig. 6) are significantly high. Besides there are several other deposits, such as Dongping orogenic Au deposit and Panasqueira W-Sn deposit, have high $^3$He/$^4$He ratios (Mao et al., 2003; Burnard and Polya, 2004). Mao et al. (2003) suggested that the high $^3$He/$^4$He (0.3–5.2 $R_a$) in the ore forming fluid of Dongping Au deposit indicate that ore-forming fluid is dominantly sourced within the mantle, however, there is another hydrothermal fluid that is magmatic origin but unrelated to the main mineralization. Burnard and Polya (2004) proposed that the high $^3$He/$^4$He in ore fluids from the Panasqueira W-Sn deposit reflected the direct addition of mantle-derived He to the ore-fluids, and suggested that they were unrelated to the granite that was spatially and temporally associated with the deposits.

The Zijinshan Cu-Au deposit and Wuziqilong Cu deposits are spatially and temporally associated with early Cretaceous granodiorite and volcanic rocks (Jiang et al., 2013; Li and Jiang, 2014; Zhang et al., 2003), which were generated above subducting Pacific plate (Jiang et al., 2013; Li and Jiang, 2014). The Sr-Nd-Hf-Pb isotopic compositions of Luoboling and Zhongliao granodiorites show a subduction-modified mantle origin, which is associated with slab-derived fluids or melts

(Chen et al., 2008; Meng et al., 2012), with assimilation of ancient crustal materials (Li and Jiang, 2014). So the felsic magmas are unlikely be the source of the high $^3$He/$^4$He, because the assimilation of ancient crustal materials produces low $^3$He/$^4$He ratios. Thus the high $^3$He/$^4$He may be the result of direct intrusion of mantle-derived volatiles. This is consistent with the presence of contemporaneous mafic dykes in the Zijinshan orefield. The mafic reservoir can keep a prolonged thermal condition, resulting in a long-lived, continuous fertilization of the shallow magmatic-hydrothermal systems (Chiaradia et al., 2009), which may be the key point of generating large porphyry-epithermal ore system in Zijinshan orefield. Underplating by mafic magmas, providing the high heat flux, volatiles, as well as metal to the ore-forming fluids without transport in felsic magma, may be a common phenomenon in giant porphyry and related epithermal deposits (Hattori, 1993, 1996; Hattori and Keith, 2001).

Porphyry Cu systems are generated mainly in compressional tectonic settings (Sillitoe, 2010), strongly extensional settings appear to lack significant porphyry Cu systems (Sillitoe, 1999; Tosdal and Richards, 2001). However, the Zijinshan orefield was formed under strongly extensional tectonic regime, evidenced by the coexistence of A-type granites, highly fractionated I-type granites and bimodal volcanic rocks during the Mid-Late Cretaceous (107–86 Ma) in Southeast China (Li et al., 2014; Zhou et al., 2006). The main factor controlling formation of porphyry Cu deposits may not be the tectonic settings but the conditions necessary to generate mafic reservoirs in the depth.

## 4. Conclusions

The ore-forming fluids of the Zijinshan Cu-Au deposit and Wuziqilong Cu deposit were a mixture of shallow crustal fluid containing crustal $^4He$ and near atmospheric Ar and magmatic fluid that contains a significant proportion of gases from the mantle. The crustal fluid was low temperature meteoric fluid that interacted with crustal rocks. The high $^3He/^4He$ ratio of magmatic fluid indicates at least 80% of the He in the magmatic fluid was derived from the mantle. The high $^3He/Q$ of the mineralizing fluids ($0.07 \times 10^{-12}$ to $8.35 \times 10^{-12}$ cm$^3$ STP J$^{-1}$) and near MORB $^3He/^{40}Ar*$ ratios suggest that the hydrothermal fluids derived heat and volatiles from the magma through advection rather than conduction which will lead to low $^3He/Q$ and $^3He/^{40}Ar*$ ratios. The absence of clear relationship between $^{40}Ar/^{36}Ar$ and $^3He/^{36}Ar$ vs $\delta^{34}S$ suggests that S is primarily derived from magma and crustal fluid doesn't supply significant S to the ore-forming system. Volatile, heat and metals (if not all at least part) may derive directly from underplating mafic magma.

## References

Baker, E.T., Lupton, J.E., 1990. Changes in submarine hydrothermal $^3He$/heat ratios as an indicator of magmatic/tectonic activity. Nature 346, 556–558.

Burnard, P.G., Polya, D.A., 2004. Importance of mantle-derived fluids during granite associated hydrothermal circulation: He and Ar isotopes of ore minerals from Panasqueira. Geochim. Cosmochim. Acta 68, 1607–1615.

Burnard, P.G., Farley, K.A., Turner, G., 1998. Multiple fluid pulses in a Samoan harzburgite. Chem. Geol. 147, 99–114.

Burnard, P.G., Hu, R.Z., Turner, G., Bi, X.W., 1999. Mantle, crustal and atmospheric noble gases in Ailaoshan gold deposits, Yunnan Province, China. Geochim. Cosmochim. Acta 63, 1595–1604.

Burnham, C.W., 1979. Magmas and hydrothermal fluids. In: Barnes, H.L. (Ed.), Geochemistry of Hydrothermal Ore Deposits. Wiley, New York, pp. 71–136.

Chen, C.H., Lee, C.Y., Shinjo, R., 2008. Was there Jurassic Paleo-Pacific subduction in South China: constraints from $^{40}Ar/^{39}Ar$ dating, elemental and Sr-Nd-Pb isotopic geochemistry of the Mesozoic basalts. Lithos 106, 83–92.

Chen, J., Chen, Y.J., Zhong, J., Sun, Y., Li, J., Qi, J.P., 2011. Fluid inclusion study of the Wuziqilong Cu deposit in the Zijinshan ore field, Fujian province. Acta Petrol. Sin. 27, 1425–1438 (in Chinese with English abstract).

Chiaradia, M., Merino, D., Spikings, R., 2009. Rapid transition to long-lived deep crustal magmatic maturation and the formation of giant porphyry-related mineralization (Yanacoch, Peru). Earth Planet. Sci. Lett. 288, 505–515.

Chiaradia, M., Ulianov, A., Kouzmanov, K., Beate, B., 2012. Why large porphyry Cu deposits like high Sr/Y magmas? Sci Rep 2, 685.

Davidheiser-Kroll, B., Stuart, F.M., Boyce, A.J., 2014. Mantle heat drives hydrothermal fluids responsible for carbonate-hosted base metal deposits: evidence from $^3He/^4He$ of ore fluids in the Irish Pb-Zn ore district. Mineral. Deposita 49, 547–553.

Eastoe, C.J., 1983. Sulfur isotope data and the nature of the hydrothermal systems at the Panguna and Frieda porphyry copper deposits, Papua New Guinea. Econ. Geol. 78, 201–213.

Field, C.W., Gustafson, L.B., 1976. Sulfur isotopes in the porphyry copper deposit at El Salvador, Chile. Econ. Geol. 71, 1533–1548.

Foeken, J.P.T., Day, S., Stuart, F.M., 2009. Cosmogenic $^3He$ exposure dating of the quaternary basalts from Fogo, Cape Verdes: implications for rift zone and magmatic reorganization. Quat. Geochron. 4, 37–49.

Gautheron, C., Moreira, M., 2002. Helium signature of the subcontinental lithospheric mantle. Earth Planet. Sci. Lett. 199, 39–47.

Graham, D.W., 2002. Noble gas isotope geochemistry of mid-ocean ridge and ocean island basalts: characterization of mantle source reservoirs. Rev. Mineral. Geochem. 47, 247–317.

Graupner, T., Niedermann, S., Kempe, U., Klemd, R., Bechtel, A., 2006. Origin of ore fluids in the Muruntau gold system: constraints from noble gas, carbon isotope and halogen data. Geochim. Cosmochim. Acta 70, 5356–5370.

Graupner, T., Niedermann, S., Rhede, D., Kempe, U., Seltmann, R., Williams, C.T., Klemd, R., 2010. Multiple sources for mineralizing fluids in the Charmitan gold(-tungsten)

mineralization (Uzbekistan). Mineral. Deposita 45, 667–682.

Hattori, K.H., 1993. High-sulfur magma, a product of fluid discharge from underlying mafic magma: evidence from Mount Pinatubo, Philippines. Geology 21, 1083–1086.

Hattori, K.H., 1996. Occurrence of sulfide and sulfate in the 1991 Pinatubo eruption products and their origin. In: Newhall, C.G., Punongbayan, R.S. (Eds.), Fire and mud: Eruptions and Lahars of Mount Pinatubo, Philippines. University of Washington Press, Seattle, pp. 807–824.

Hattori, K.H., Keith, J.D., 2001. Contribution of mafic melt to porphyry copper mineralization: evidence from Mount Pinatubo, Philippines, and Bingham Canyon, Utah, USA. Miner. Deposita 36, 799–806.

Hayba, D.O., Ingebritsen, S.E., 1997. Multiphase groundwater flow near cooling plutons. J. Geophys. Res. 102, 12235–12252.

Hu, R.Z., Zhou, M.F., 2012. Multiple Mesozoic mineralization events in South China-an introduction to the thematic issue. Mineral. Deposita 47, 579–588.

Hu, R.Z., Burnard, P.G., Turner, G., Bi, X.W., 1998a. Helium and argon systematics in fluid inclusions of Machangqing copper deposit in west Yunnan province, China. Chem. Geol. 146, 55–63.

Hu, R.Z., Turner, G., Burnard, P.G., Zhong, H., Ye, Z.J., Bi, X.W., 1998b. Helium and argon isotopic geochemistry of Jinding superlarge Pb-Zn deposit. Sci. Chin. Ser. D 41, 442–448.

Hu, R.Z., Burnard, P.G., Bi, X.W., Zhou, M.F., Peng, J.T., Su, W.C., Wu, K.X., 2004. Helium and argon isotope geochemistry of alkaline intrusion-associated gold and copper deposits along the Red River-Jinshajiang fault belt, SW China. Chem. Geol. 203, 305–317.

Hu, R.Z., Burnard, P.G., Bi, X.W., Zhou, M.F., Peng, J.T., Su, W.C., Zhao, J.H., 2009. Mantle-derived gaseous components in ore-forming fluids of the Xiangshan uranium deposit, Jiangxi province, China: evidence from He, Ar and C isotopes. Chem. Geol. 266, 86–95.

Hu, R.Z., Bi, X.W., Jiang, G.H., Chen, H.W., Peng, J.T., Qi, Y.Q., Wu, L.Y., Wei, W.F., 2012. Mantle-derived noble gases in ore-forming fluids of the granite-related Yaogangxian tungsten deposit, Southeastern China. Miner. Deposita 47, 623–632.

Imai, A., Listanco, E.L., Fujii, T., 1993. Petrologic and sulfur isotopic significance of highly oxidized and sulfur-rich magma of Mt. Pinatubo, Philippines. Geology 21, 699–702.

Jean-Baptiste, P., Bougault, H., Vangriesheim, A., Charlou, J.L., Raford-Knoery, J., Fouquet, Y., Needham, D., German, C., 1998. Mantle $^3He$ in hydrothermal vents and plume of the lucky strike site (MAR 37°17′) and associated geothermal heat flux. Earth Planet. Sci. Lett. 157, 69–77.

Jiang, S.H., Liang, Q.L., Bagas, L., Wang, S.H., Nie, F.J., Liu, Y.F., 2013. Geodynamic setting of the Zijinshan porphyry-epithermal Cu-Au-Mo-Ag ore system, SW Fujian Province, China: constrains from the geochronology and geochemistry of the igneous rocks. Ore Geol. Rev. 53, 287–305.

Jiang, S.H., Bagas, L., Liang, Q.L., 2015. New insights into the petrogenesis of volcanic rocks in the Shanghang Basin in the Fujian Province, China. J. Asian Earth Sci. 105, 48–67.

Kendrick, M.A., Burgess, R., Pattrick, R.A., Turner, G., 2001. Fluid inclusion noble gas and halogen evidence on the origin of Cu porphyry mineralizing fluids. Geochim. Cosmochim. Acta 65, 2651–2668.

Kendrick, M.A., Burgess, R., Pattrick, R.A., Turner, G., 2002. Hydrothermal fluid origins in a fluorite-rich Mississippi valley-type district; combined noble gas (He, Ar, Kr) and halogen (Cl, Br, I) analysis of fluid inclusions from the South Pennine ore field, United Kingdom. Econ. Geol. 97, 435–451.

Kendrick, M.A., Burgess, R., Harrison, D., Bjorlykke, A., 2005. Noble gas and halogen evidence for the origin of Scandinavian sandstone-hosted Pb-Zn deposits. Geochim. Cosmochim. Acta 69, 109–129.

Kennedy, B.M., Hiyagon, H., Reynolds, J.H., 1991. Noble gases from Honduras geothermal sites. J. Vocanol Geotherm. Res. 45, 29–39.

Kyser, T.K., 1990. Stable isotopes in the continental lithospheric mantle. In: Menzies, M.A. (Ed.), Continental Mantle. Clarendon Press, Oxford, pp. 127–156.

Lee, J.Y., Marti, K., Severinghaus, J.P., Kawamura, K., Yoo, H.S., Lee, J.B., Kim, J.S., 2006. A redetermination of the isotopic abundances of atmospheric Ar. Geochim. Cosmochim. Acta 70, 4507–4512.

Li, B., Jiang, S.Y., 2014. A subduction-related metasomatically enriched mantle origin for the Luoboling and Zhongliao Cretaceous granitoids from South China: implications for magma evolution and Cu-Mo mineralization. Int. Geol. Rev. 57 (9–10), 1239–1266.

Li, Z.L., Hu, R.Z., Yang, J.S., Peng, J.T., Li, X.M., Bi, X.W., 2007. He, Pb and S isotopic constraints on the relationship between the A-type Qitianling granite and the Furong tin deposit, Hunan Province, China. Lithos 97, 161–173.

Li, X.F., Wang, C.Z., Hua, R.M., Wei, X.L., 2010. Fluid origin and structural enhancement during mineralization of the Jinshan orogenic gold deposit, South China. Mineral. Deposita 45, 583–597.

Li, J.H., Zhang, Y.Q., Dong, S.W., Johnston, S.T., 2014. Cretaceous tectonic evolution of South China: a preliminary synthesis. Earth-Sci. Rev. 134, 98–136.

Liang, Q.L., Jiang, S.H., Wang, S.H., Li, C., Zeng, F.G., 2012. Re-Os dating of molybdenite from the Luoboling porphyry Cu-Mo deposit in the Zijinshan ore field of Fujian province and its geological significance. Acta Geol. Sin. 86, 1113–1118 (in Chinese with English abstract).

Liu, X.D., Hua, R.M., 2005. $^{40}Ar/^{39}Ar$ dating of adularia from the Bitian gold-silver-copper deposit, Fujian province. Geol. Rev. 51, 151–155 (in Chinese with English abstract).

Liu, W.Y., Nigel, J.C., Cristiana, L.C., Liu, Y., Qiu, X.P., Chen, Y.C., 2016. Mineralogy of tin-sulfides in the Zijinshan porphyry-epithermal system, Fujian Province, China. Ore Geol. Rew. 72, 682–698.

Lupton, J.E., Baker, E.T., Massoth, G.J., 1989. Variable $^3He$/heat ratios in submarine hydrothermal systems: evidence from two plumes over the Juan de Fuca ridge.

Nature 337, 161–164.

Lupton, J.E., Baker, E.T., Massoth, G.J., Thomson, R.E., Burd, B.J., Butterfield, D.A., Embley, R.W., Cannon, G.A., 1995. Variations in water-column $^3$He/heat ratios associated with the 1993 CoAxial event, Juan de Fuca Ridge. Geophys. Res. Lett. 22, 155–158.

Mao, J.W., Li, Y.Q., 2003. Fluid inclusion and noble gas studies of the Dongping gold deposit, Hebei province, China: a mantle connection for mineralization? Econ. Geol. 98, 517–534.

Mao, J.W., Cheng, Y.B., Chen, M.H., Franco, P., 2013. Major types and time–space distribution of Mesozoic ore deposits in South China and their geodynamic settings. Mineral. Deposita 48, 264–267.

Meng, L.F., Li, Z.X., Chen, H.L., Li, X.H., Wang, X.C., 2012. Geochronological and geochemical results from Mesozoic basalts in southern South China Block support the flat-slab subduction model. Lithos 132-133, 127–140.

Morelli, R., Creaser, R.A., Seltmann, R., Stuart, F.M., Selby, D., Graupner, T., 2007. Age and source constraints for the giant Muruntau gold deposit, Uzbekistan, from coupled Re-Os-He isotopes in arsenopyrite. Geology 35, 795–798.

Norman, D.I., Musgrave, J.A., 1994. N$_2$-He-Ar composition in fluid inclusion: indicators of fluid source. Geochim. Cosmochim. Acta 58, 1119–1132.

Ohmoto, H., Goldhaber, M.B., 1997. Sulfur and carbon isotopes. In: Barnes, H.L. (Ed.), Geochemistry of Hydrothermal Ore Deposits, 3rd ed. Wiley, New York, pp. 517–611.

O'Nions, R.K., Oxburgh, E.R., 1983. Heat and helium in the earth. Nature 306, 429–431.

Pettke, T., Frei, R., Kramers, J.D., Villa, I.M., 1997. Isotope systematics in vein gold from Brusson, Val d'Ayas (NW Italy) 2. (U + Th)/He and K/Ar in native Au and its fluid inclusions. Chem. Geol. 135, 173–187.

Poreda, R.J., Arnórsson, S., 1992. Helium isotopes in Icelandic geothermal systems: II. Helium-heat relationships. Geochim. Cosmochim. Acta 56, 4229–4235.

Porter, T.M., 2005. Super Porphyry Copper & Gold Deposits—A Global Perspective. PGC Publishing, Adelaide.

Sánchez, V., Stuart, F.M., Martín-Crespo, T., Vindel, E., Corbella, M., Cardellach, E., 2010. Helium isotopic ratios in fluid inclusions from fluorite-rich Mississippi Valley-type district of Asturias, northern Spain. Geochem. J. 44 (6), E1–E4.

Sheppard, S.M.F., Taylor, H.P., 1974. Hydrogen and oxygen isotope evidence for the origins of water in the Boulder Batholith and the Butte ore deposits. Montana. Econ. Geol. 69, 926–946.

Sillitoe, R.H., 1997. Characteristics and controls of the largest porphyry copper-gold and epithermal gold deposits in the circum-Pacific region. Aust. J. Earth Sci. 44, 373–388.

Sillitoe, R.H., 1999. VMS and porphyry copper deposits: products of discrete tectono-magmatic settings. In: Stanley (Ed.), Mineral Deposits: Processes to Processing. Balkema, Rotterdam, pp. 7–10.

Sillitoe, R.H., 2010. Porphyry copper systems. Econ. Geol. 105, 3–41.

Simmons, S.F., Sawkins, F.J., Schlutter, D.J., 1987. Mantle-derived helium in two Peruvian hydrothermal ore deposits. Nature 329, 429–432.

Smith, P.E., Evensen, N.M., York, D., Szatmari, P., Oliveira, D.C., 2001. Single-crystal $^{40}$Ar-$^{39}$Ar dating of pyrite: no fool's clock. Geology 29, 403–406.

So, C.S., Zhang, D.Q., Yun, S.T., Li, D.X., 1998. Alteration-mineralization zoning and fluid inclusions of the high sulfidation epithermal Cu-Au mineralization at Zijinshan, Fujian Province, China. Econ. Geol. 93, 961–980.

Stuart, F.M., Turner, G., 1992. The abundance and isotopic composition of the noble gases in ancient fluids. Chem. Geol. 101, 97–109.

Stuart, F.M., Turner, G., Duckworth, R.C., Fallick, A.E., 1994a. Helium isotopes as tracers

of trapped hydrothermal fluids in ocean-floor sulfides. Geology 22, 823–826.

Stuart, F.M., Turner, G., Taylor, R.P., 1994b. He-Ar systematics of ancient hydrothermal fluids: resolving mantle and crustal contributions. In: Matsuda, J.I. (Ed.), Noble Gas Isotope Geochemistry & Cosmochemistry. Terra Publishing, Japan, pp. 261–278.

Stuart, F.M., Burnard, P.G., Taylor, R.P., Turner, G., 1995. Resolving mantle and crustal contributions to ancient hydrothermal fluids: He-Ar isotopes in fluid inclusions from DaeHwa W-Mo mineralisation, South Korea. Geochim. Cosmochim. Acta 59, 4663–4673.

Sun, W.D., Arculus, R.J., Kamenetsky, V.S., Binns, R.A., 2004. Release of gold-bearing fluids in convergent margin magmas promoted by magnetite crystallization. Nature 431, 975–978.

Tang, Y.Y., Bi, X.W., Fayek, M., Stuart, F.M., Wu, L.Y., Jiang, G.H., Xu, L.L., Liang, F., 2017. Origin of the Jinding Zn-Pb deposit, Northwest Yunnan province, China: constraints from rare earth elements and noble gas isotopes. Ore Geol. Rew. http://dx.doi.org/10.1016/j.oregeorev.2017.04.024.

Torgersen, T., Kennedy, B.M., Hiyagon, H., 1988. Argon accumulation and the crustal degassing flux of $^{40}$Ar in the Great Artesian Basin, Australia. Earth Planet. Sci. Lett. 92, 43–56.

Tosdal, R.M., Richards, J.P., 2001. Magmatic and structural controls on the development of porphyry Cu ± Mo ± Au deposits. Rev. Econ. Geol. 14, 157–181.

Turner, G., Stuart, F.M., 1992. Helium/heat ratios and deposition temperatures of sulfides from the ocean floor. Nature 357, 581–583.

Turner, G., Burnard, P., Ford, J.L., Gilmour, J.D., Lyon, I.C., Stuart, F.M., 1993. Tracing fluid sources and interactions. Phil. Trans. R. Soc. Lond. A. 344, 127–140.

Wallace, P., Carmichael, I.S.E., 1992. Sulfur in basaltic magmas. Geochim. Cosmochim. Acta 56, 1863–1874.

Wei, H.X., Sun, X.M., Zhai, W., Shi, G.Y., Liang, Y.H., Mo, R.W., Han, M.X., Yi, J.Z., 2010. He-Ar-S isotopic compositions of ore-forming fluids in the Bangbu large-scale gold deposit in southern Tibet, China. Acta Petrol. Sin. 26, 1685–1691.

Wu, L.Y., Hu, R.Z., Peng, J.T., Bi, X.W., Jiang, G.H., Chen, H.W., Wang, Q.Y., Liu, Y.Y., 2011. He and Ar isotopic compositions and genetic implications for the giant Shizhuyuan W-Sn-Bi-Mo deposit, Hunan Province, South China. Int. Geol. Rev. 53, 677–690.

Wu, L.Y., Hu, R.Z., Qi, Y.Q., Zhu, J.J., 2013. Zircon LA-ICP-MS U-Pb ages and geochemical characteristics of quartz syenite porphyry from Jintonghu deposit in Zijinshan ore field, Fujian Province, South China. Acta Petrol. Sin. 29, 4151–4166 (in Chinese with English abstract).

York, D., Masliwec, A., Kuybida, P., Hanes, J.E., Hall, C.M., Kenyon, W.J., Spooner, E.T.C., Scott, S.D., 1982. $^{40}$Ar/$^{39}$Ar dating of pyrite. Nature 300, 52–53.

Zhang, D.Q., Li, D.X., Zhao, Y.M., Chen, J.H., Li, Z.L., Zhao, K.D., 1992. Alteration and Mineralization Zoning of the Zijinshan Copper-Gold Deposit. Geological Publishing House, Beijing (in Chinese with English abstract).

Zhang, D.Q., Yu, H.Q., Li, D.X., Feng, C.Y., 2003. The porphyry-epithermal metallogenic system in the Zijinshan region, Fujian province. Acta Geol. Sin. 77, 253–261 (in Chinese with English abstract).

Zhong, J., Chen, Y.J., Pirajno, F., Chen, J., Li, J., Qi, J.P., Li, N., 2014. Geology, geochronology, fluid inclusion and H-O isotope geochemistry of the Luoboling porphyry Cu-Mo deposit, Zijinshan Orefield, Fujian Province. China. Ore Geol. Rev. 57, 61–77.

Zhou, X.M., Sun, T., Shen, W.Z., Shu, L.S., Niu, Y.L., 2006. Petrogenesis of Mesozoic granitoids and volcanic rocks in South China: a response to tectonic evolution. Episodes 29, 21–26.